DOI: 10.1002/chem.200500287

Elongated Dihydrogen Versus Compressed Dihydride Complexes: The Temperature Dependence of the H–D Spin–Spin Coupling Constant as a Criterion To Distinguish between Them

Ricard Gelabert, Miquel Moreno, and José M. Lluch*[a]

Abstract: To be able to propose experimental tests to distinguish elongated dihydrogen transition-metal complexes from compressed dihydride transition-metal complexes, a thorough density functional study of the electronic structure in combination with quantum nuclear dynamics calculations have been performed for complexes $[Cp^*Ru(H_2PCH_2PCH_2(H_2)]^+$ and $[CpRe(CO)_2H_2]$. The results of this study suggest that elongated dihydrogen complexes and compressed dihydride complexes have different properties and that it should be possible to distinguish between them experimentally. In particular, different behavior is predicted with respect to 1) the sign of the isotope geometric effect on the H–H distance at 0 K, 2) the temperature dependence of the H–H distance, and 3) the temperature dependence of the H–D spin–spin coupling constant in ^1H NMR spectroscopy.

Keywords: density functional calculations · dihydride complexes · dihydrogen complexes · spin–spin coupling constants · transition metals

Introduction

Among the wide variety of transition-metal complexes that include hydrogen atoms in the coordination sphere of the metal, stretched or elongated dihydrogen complexes have aroused enduring interest despite their scarcity.[1] With a H–H distance between 1.0 Å and 1.5 Å, stretched dihydrogen complexes can be envisaged as arrested intermediates in the important process of oxidative addition of a hydrogen molecule to a metal atom, a process of great relevance in catalysis.

Aside from their relevance in catalytic studies, the persisting interest in stretched dihydrogen complexes is partly attributable to their surprising and certainly unique properties. Contrary to what has been reported for "classical" dihydride complexes ($R_{H-H} > 1.5$ Å) and "nonclassical" dihydrogen complexes ($R_{H-H} < 1.0$ Å), stretched dihydrogen complexes show a clear temperature dependence of the spin–spin coupling constant in NMR experiments in which the H_2 ligand has been substituted by HD ($^1J_{HD}$). Moreover, and surprisingly enough for a family of complexes with so few members, different opposing behaviors have been observed: $^1J_{HD}$ either increases or decreases with temperature. By virtue of a well-established inverse relationship between $^1J_{HD}$ and R_{H-H},[2] this temperature dependence of $^1J_{HD}$ has found prompt interpretation in terms of shortening or lengthening of R_{H-H} with temperature.

After several unsuccessful attempts, satisfactory explanation was provided for this behavior in the stretched dihydrogen complex $[Cp^*Ru(dppm)(H_2)]^+$ (dppm = bisdiphenylphosphinomethane) (**1**) (R_{H-H} = 1.10 Å, neutron diffraction[3]), by means of combined quantum nuclear dynamics calculations on a density functional theory (DFT) surface.[4] The substantial anharmonicity of the potential energy surface (PES) that describes the internal motion in the $Ru-H_2$ unit, together with the varying thermal population of excited vibrational states could explain the geometry obtained by neutron diffraction and the lengthening of R_{H-H}, observed indirectly through a decrease in the value of $^1J_{HD}$ with temperature. The adequacy of this theoretical explanation was put to the test when it predicted a systematic shortening of the H–H distance for heavier isotopomers of the dihydrogen ligand coordinated in the complex, a prediction that was afterwards proven to be true.[5,6] As such, stretched dihydrogen complexes could be understood and set aside from the broad family of nonclassical dihydrogen complexes as a group with specific properties attributed to a common cause: the effects of the anharmonicity of the PES on the vibrational eigenstates of the $M-H_2$ unit in the complex.

[a] Dr. R. Gelabert, Dr. M. Moreno, Prof. Dr. J. M. Lluch
Universitat Autònoma de Barcelona
Departament de Química
08193 Bellaterra, Barcelona (Spain)
Fax: (+34) 935-812-920
E-mail: lluch@klingon.uab.es

Recently, Pons and Heinekey reported the synthesis and characterization of the complex $[Cp^*Ir(dmpm)H_2]^{2+}$ (dmpm = bis(dimethyl)phosphinomethane) (**2**).[7] This complex was first described as a stretched dihydrogen complex, in which $^1J_{HD}$ increased with the temperature, which has a comparatively large R_{H-H} distance of 1.49 Å, estimated from $T_{1(min)}$ relaxation time measurements. In a subsequent theoretical study, it was found that its PES had two minima, the most stable one matching the description of a dihydride (R_{H-H} = 1.63 Å).[8] A simplified one-dimensional nuclear dynamics study described the geometry of the Ir–H_2 unit and also showed that the mean thermal R_{H-H} decreased with increasing temperature, thus indirectly explaining the experimental observations. The fact that the most stable minimum on the Born–Oppenheimer potential energy surface (i.e. before nuclear motion was considered) was that of a dihydride complex, and that the vibrational states indicated progressively shorter H–H distances, suggested that this complex could be described as a "compressed dihydride" rather than stretched dihydrogen. Very recently, complex **2** has been the target of a thorough dynamical study in which an anharmonic vibrational analysis was performed.[9] More importantly, the dynamical study combined with a first-principles theoretical determination of both the ^{1}H NMR chemical shift and the $^1J_{HD}$ surfaces describes almost quantitatively the temperature dependence of $^1J_{HD}$ without resorting to correlations of any kind. This result further validates the hypothesis behind the explanation of the strange properties of this kind of complexes.

Other complexes have been reported with properties mimicking those of **2**. Some years ago, Casey et al. reported the synthesis and characterization of the complex $[CpRe(CO)_2H_2]$ (**3**), described as a dihydride complex with a temperature-dependent $^1J_{HD}$ value (increasing with temperature).[10] An equilibrium between the *cis*-dihydride and a hypothetical dihydrogen species was postulated; however, attempts to detect the dihydrogen isomer by low-temperature IR spectroscopy were fruitless. To our knowledge, **3** has not yet been studied theoretically to explain its properties. In view of recent developments it now seems likely that complex **3** belongs to the stretched dihydrogen family of complexes.

At this point, it is logical to wonder whether the term "compressed dihydride" could be more than just a descriptor for complex **2** and could apply to more cases. Accordingly, the set of complexes previously termed "stretched dihydrogen complexes" could actually be divided into two different groups with completely different properties. Herein, we will try to provide theoretical grounds in favor of such a distinction and also discuss ways to distinguish between both kinds of complexes. To tackle this task, a comparative study of two opposite cases of "stretched" dihydrogen complexes is performed. Quantum nuclear dynamics are used to determine the temperature dependence of the $^1J_{HD}$ coupling constant from first principles. As opposite cases, two stretched dihydrogen complexes with very different reported H–H distances have been selected. Complex **1** is a clear example of a "conventional" stretched dihydrogen complex and, as such, has been selected for this study. In contrast, complex **3** has been chosen because the low value of $^1J_{HD}$ seems to indicate that this complex is closer to the description of a compressed dihydride. For comparison purposes we compare our results to those published for complex $[W(CO)_3(PH_3)_2(H_2)]$ (**4**), a model of complex $[W(CO)_3(PCy_3)_2(H_2)]$, a clear dihydrogen complex.[11]

We note that the methodology used in this work to obtain the results for complex **1** differs slightly from that used for the original theoretical work.[4]

Computational Methods

Electronic structure calculations: As in the previous theoretical study,[4] complex **1** is modeled as $[Cp^*Ru(H_2PCH_2CH_2)(H_2)]^+$ (**1′**). No modeling is performed on complex **3**. For complexes **1′** and **3**, the only restriction imposed was global C_s symmetry. The GAUSSIAN 03 program was used in all electronic structure calculations.[12]

Electronic structure calculations were performed at the DFT level.[13,14] The functional chosen was the three-parameter hybrid functional of Becke, and the Lee, Yang, and Parr correlation functional, widely known as B3LYP.[15,16] To reduce the computational cost, bearing in mind the large number of point calculations needed, an effective core operator was used to replace the core electrons of the ruthenium and rhenium atoms.[17] Outer electrons were described with the basis set associated with the pseudopotential of Hay and Wadt with a standard double-ζ LANL2DZ contraction.[12,17]

The phosphorus atoms in complex **1′** were described with the LANL2DZ pseudopotential and basis set, enlarged with d polarization functions.[18] The standard split valence 6-31G(d) basis set was used for all carbon atoms.[19] All hydrogen atoms were described with the 6-31G basis set,[20] except those directly linked to the ruthenium atom, for which 6-31G(p) was used instead.[21] We note that the basis set used for **1′** differs slightly from that used in previous work.[4]

The carbon and oxygen atoms in complex **3** were described with the 6-31G(d) basis set.[19] Hydrogen atoms were treated exactly the same as for complex **1′**.

^{1}H NMR chemical shifts (δ) relative to hydrogen atoms in tetramethylsilane (TMS) were obtained from nuclear magnetic shielding tensors computed at the DFT level with the B3LYP functional and the gauge-invariant atomic orbital (GIAO) method.[12,22–24] Indirect NMR spin–spin coupling constants for H and D in the HD isotopic variant of the dihydrogen complex, $^1J_{HD}$, were determined at the DFT level with the B3LYP functional and the GIAO method.[12,25–27] The coupling constants were computed as a sum of the Fermi contact (FC), spin dipolar (SD), paramagnetic spin–orbit (PSO), and diamagnetic spin–orbit (DSO) contributions. In selected cases, $^1J_{HD}$ was computed for structures in which the hydrogen atoms bound to the metal atoms were described with the IGLO-III basis set to examine basis set convergence.[28]

Nuclear dynamics calculations: This research work is concerned with the dynamics of the M–H_2 unit (M = Re, Ru) and, because of the lightness of the hydrogen atoms, a quantum treatment is in order. To determine both energy levels and wave functions of the nuclear motion, the nuclear Schrödinger equation [Eq. (1)] has to be solved, where $\boldsymbol{R}$ is a $3N-6$ component vector describing a given arrangement of the nuclei, and U is the potential energy surface (PES), computed by adding the electronic potential energy plus internuclear repulsion energy obtained within the Born–Oppenheimer approximation (static nuclei).

$$[\hat{T}_{\text{nuclear}} + U(\boldsymbol{R})]\psi_{\text{nuclear}} = E\psi_{\text{nuclear}} \quad (1)$$

Because computation of the full $U(\boldsymbol{R})$ is unattainable, a reduction of the dimensionality that preserves the main features of the potential energy surface is needed. It has been shown elsewhere that the dynamics of the M–H_2 unit in elongated dihydrogen complexes extensively mixes the H–H and M–H_2 motions.[4,29,30,9] With this in mind, a two-dimensional surface was computed, the variables chosen being the H–H and M–H_2 distances, the latter being defined as the distance between the metal center and the point halfway between both hydrogen atoms. This choice greatly simplifies the kinetic energy operator in Equation (1).

When computing this PES, we allowed global relaxation of the complex, except for the H–H and M–H_2 distances, whilst keeping the complex within the C_s symmetry group at all times. A total of nine distance values in the M–H_2 direction and 11 in the H–H direction were computed to build a grid of 99 points, each corresponding to a different structure. This mesh of points was fitted into a two-dimensional cubic splines functional form to facilitate further calculations.[31]

The generic discrete variable representation (DVR) method proposed by Colbert and Miller was chosen to solve Equation (1).[32] The DVR representation consisted of a rectangular grid of 20×20 points. After the DVR matrix representation of the Hamiltonian is constructed, its diagonalization yields the eigenvalues (vibrational energy levels) and eigenvectors (vibrational wave functions). The wave functions are used in further calculations of the expectation values and averaged quantities, as will be described in the text. It was verified that the results remained essentially invariant upon increasing the number of points in the DVR grid.

Results and Discussion

Even though, as mentioned in the Introduction, complex **1′** has been studied theoretically with success before, the explanation of the temperature dependence of $^1J_{HD}$ was indirect and based on the well-known correlation between this magnitude and R_{H-H}.[4] Recent advances in computer power and algorithmics have made it possible to compute the value of the $^1J_{HD}$ surfaces, which imply computing $^1J_{HD}$ values for a large number of structures, with acceptable precision and reasonable use of computational resources. Incidentally, in a very recent paper, we presented a thorough study of complex **2** in which a sizeable portion of the $^1J_{HD}$ surface was computed and used to calculate vibrational state-averaged values of $^1J_{HD}$ and thus determine, from first principles, the temperature dependence of $^1J_{HD}$ by means of a Boltzmann average.[8] In this study it was found that $^1J_{HD}$ depended not only on R_{H-H}, as is well known, but also that it has a certain dependence on R_{M-H_2}. Hence we think it is preferable, if possible, to compute $^1J_{HD}$ directly and compare it to experimental data, especially since it has been previously demonstrated in several cases of elongated dihydrogen/compressed dihydride complexes that M–H_2 and H–H motions are inextricably coupled.[4,29,30,9]

The temperature dependence of $^1J_{HD}$ in complex **1** was established at the time its crystal structure was resolved by means of neutron diffraction (22.3 Hz at 213 K, 21.1 Hz at 295 K).[3] When attempting to verify the foretold[4] isotope effect on the H–H distance for **1′**, Heinekey and co-workers carried out an extensive NMR study of **1** and related complexes.[5,6] Besides verifying that there was a real isotope effect in the direction predicted (shortening H–H for heavier isotopomers of the H_2 ligand), it was found that $^1J_{HD}$ *decreased* with temperature for a whole set of complexes related to **1** and also that all these complexes had a measurable isotope effect on the chemical shift. In particular, it was determined that the chemical shift for the HD and HT isotopomers appeared 15 and 22 ppb, respectively, farther upfield than for the HH case, for measurements at 300 K in CD_2Cl_2.[6] As for complex **3**, Casey et al. determined that $^1J_{HD}$ *increased* with temperature (5.8 Hz at −35 °C and 6.5 Hz at +28 °C). We could not find a resolved structure for **3**; however, Casey et al. noted that the $^1J_{HD}$ value found was larger than any that had been reported for any metal dihydride complex and smaller than any reported for a dihydrogen complex. The use of the new correlation[8] of $^1J_{HD}$ and R_{H-H} would yield an estimated value of 1.41 Å at room temperature.

The availability of data for the isotope effect on the ^{1}H NMR chemical shift and $^1J_{HD}$ for **1** and **3** makes it possible to carry out a parallel study for both complexes similar to that recently published for complex **2**.[9] Hence, the study begins with a search for the stationary points in the dihydrogen or dihydride regions of the complete configurational space for **1′** and **3**. Next, the two-dimensional potential energy surface within the Born–Oppenheimer approximation as a function of the H–H and M–H_2 stretches will be built. Furthermore, the ^{1}H NMR chemical shift and $^1J_{HD}$ coupling constant surfaces will also be built. Finally, quantum dynamics calculations will be performed for both complexes to determine the temperature dependence of $^1J_{HD}$ and the chemical shift.

Static studies: The stationary points of complexes **1′** and **3** corresponding to the minima have been located and characterized within the global C_s symmetry by direct minimization of the Born–Oppenheimer potential energy surface.

The geometries of these stationary points with respect to the $M-H_2$ units are detailed in Table 1. We note that the change in basis set has not had any important effects on the geometry of complex **1′**.[4] From a purely electronic point of view, that is, before nuclear motion is considered, complex **1′** can properly be described as a dihydrogen complex, whereas complex **3** fits the description of a dihydride. However, as is known for this family of complexes, the experimentally resolved geometry cannot be compared directly to that of a direct minimization of the potential energy, as is customary with most other systems, because the flatness of the potential energy surface describing the motion within the $M-H_2$ unit makes it necessary to consider nuclear motion quantum dynamically. Thus, following the same procedure as in previous studies[4,29,8] we determined the relaxed potential energy surface as a function of H–H and $M-H_2$ stretches, which are represented in Figure 1.

Table 1. Geometries of the minimum energy structures of the $M-H_2$ unit in some theoretically studied, stretched dihydrogen complexes. For complex **2**, data shown corresponds to the lowest energy minimum.

Complex	No.	R_{H-H} [Å]	R_{M-H_2} [Å]	Reference
$[W(CO)_3(PH_3)_2(H_2)]$	**4**	0.83	1.87	[11]
$[Cp^*Ru(H_2PCH_2PH_2)(H_2)]^+$	**1′**	0.88	1.67	this work
$[CpRe(CO)_2H_2]$	**3**	1.60	1.45	this work
$[Cp^*Ir(dmpm)H_2]^{2+}$	**2**	1.63	1.37	[8]

For complexes having minima so different to each other it is remarkable that their PESes share so many traits. The overall shape of the PES is the same, with a deep energetic "cleft" following a rather straight path, along which the $M-H_2$ distance decreases while H–H increases. This has been the case in all complexes of this family we have studied so far and is at the root of the dynamical nonseparability of the H–H and $M-H_2$ stretches that happens in these complexes once the hydrogen molecule is coordinated to the metal center. It is illuminating to compare these PESes to other available examples. Complex $[W(CO)_3(PH_3)_2(H_2)]$ (**4**) was exhaustively studied to model the thermodynamics of the dihydrogen–dihydride equilibrium in $[W(CO)_3(PCy_3)_2(H_2)]$, one of the so-called Kubas complexes, and as such, a clear dihydrogen complex.[11] At the dihydride end, we have studied recently the compressed dihydride complex **2**, which, in terms of the minimum of its PES, is a dihydride. Geometric data for complexes **2** and **4** are also collected in Table 1 and the corresponding potential energy surfaces in Figure 1. All the PESes display a strong family resemblance in the form of this above-mentioned energy cleft, even in the case of complex **4**, which, strictly speaking, does not belong to this family of complexes. Actually, the only relevant difference seems to lie in the position of the deepest point of the profile in the general path along which R_{H-H} lengthens and R_{M-H_2} shortens.

The values of δ and $^1J_{HD}$ for the minimum energy structures of **1′** and **3** are given in Table 2. Even though the values in Table 2 do not completely agree with experimental data, it should be remembered that the former values are

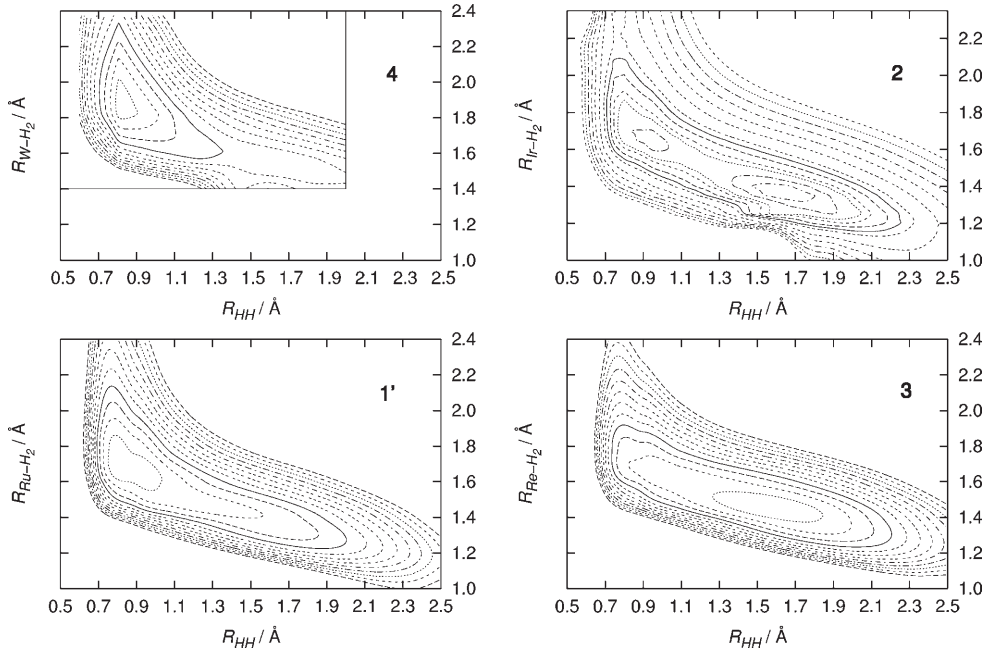

Figure 1. Contour plots of the relaxed potential energy surfaces for complexes **1′** (bottom left) and **3** (bottom right). For comparison, the corresponding potential energy surfaces for complexes **4**[11] (top left) and **2**[8] (top right) are also included. To make the comparison meaningful, all surfaces are defined on the same range of H–H and $M-H_2$ distances. Energy contours start at 1 kcal mol^{-1} and increase in 2 kcal mol^{-1} intervals. Dihydride character increases counterclockwise, starting at complex **4** (top left).

Table 2. ^{1}H NMR parameters for complexes **1′** and **3** computed for the minimum energy structure.

Complex	δ [ppm]	$^1J_{HD}$ [Hz]
1′	−5.213	34.7
3	−6.057	2.91

those for a single structure—that of the minimum—and that a comparison with experimental data should be based on the Boltzmann average of state-averaged values of δ and $^1J_{HD}$. In any event, the values of $^1J_{HD}$ for the minimum of **1′** are reasonable for a dihydrogen complex, and those of **3** are reasonable for a dihydride complex. To estimate the measured values of the ^{1}H NMR chemical shift and $^1J_{HD}$, the corresponding surfaces were computed and are depicted in Figure 2 and Figure 3, respectively.

Figure 2 and Figure 3 reveal a surprising fact: even though the absolute value of the chemical shift and $^1J_{HD}$ may differ, the general shape of these surfaces is the same for both complexes. Furthermore, comparison to Figure 3 in reference [9] clearly shows that the ^{1}H NMR chemical shift surfaces for complexes **1′**, **2**, and **3** look very much alike. The form of the chemical shift surface is the same in all complexes; however, there is a certain constant point-to-point shift for complex **1′** downfield of **3**. This is reasonable in view of the fact that **1′** is actually a cationic complex, hence it has less electron density and consequently it seems reasonable that the H_2 ligand is less shielded.

Something similar happens to the $^1J_{HD}$ surfaces (compare Figure 3 in this work and Figure 2 in reference [9]). This indicates that $^1J_{HD}$ is mainly a function of the geometry and that complexes with similar geometries of the M–H_2 unit, not only H–H, ought to have similar values of $^1J_{HD}$. This fact is implicit in the known correlations of $^1J_{HD}$ and R_{H-H}. We note also that $^1J_{HD}$ is not only a function of R_{H-D}, but also of R_{M-HD}. Therefore, according to these computations, differences in $^1J_{HD}$ detected at the experimental level depend on the underlying potential energy surface (which indicates where the minimum is and how the vibrational energy levels are).

It is known that the accuracy of theoretically computed spin–spin coupling constants and nuclear shielding constants greatly depends on the quality of the basis sets. Large basis sets are known to be necessary for nuclear shielding constants.[33] As for spin–spin coupling constants, in addition to a large basis set requirement, the dominance of the Fermi-contact contribution requires a proper description of the nuclear region. In the case of hydrogen atoms, this means using 1s functions with large exponents.[33,34] Excellent performance has been reported for both nuclear shielding and spin–spin coupling constants with the larger basis sets of Schindler and Kutzelnigg, or IGLO basis sets, which are of triple-ζ quality or better.[28] However, the dynamical nature of the study we present here requires the computation of δ and $^1J_{HD}$ for a large number of different structures, which would turn out to be too costly with these large basis sets. Instead, to validate the basis set convergence of the δ and $^1J_{HD}$ surfaces computed so far, we computed these magni-

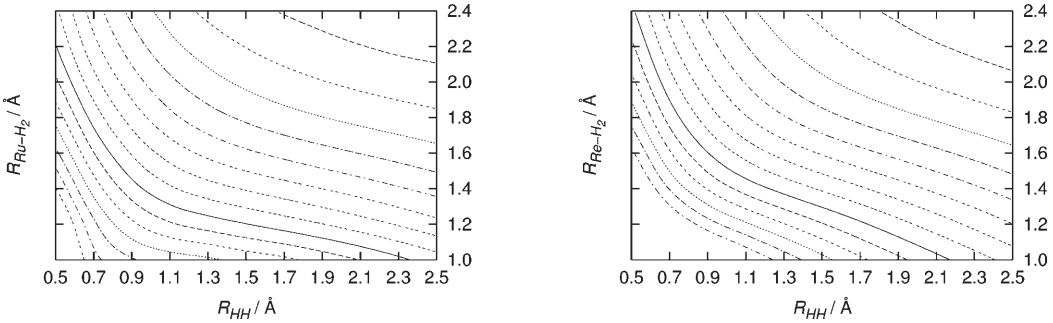

Figure 2. Contour plots of the ^{1}H NMR chemical shift relative to TMS (31.775 ppm at this level of calculation) for complexes **1′** (left) and **3** (right). Contours start at $\delta = -20$ ppm (contour at bottom left in both cases) and increase in 2 ppm intervals.

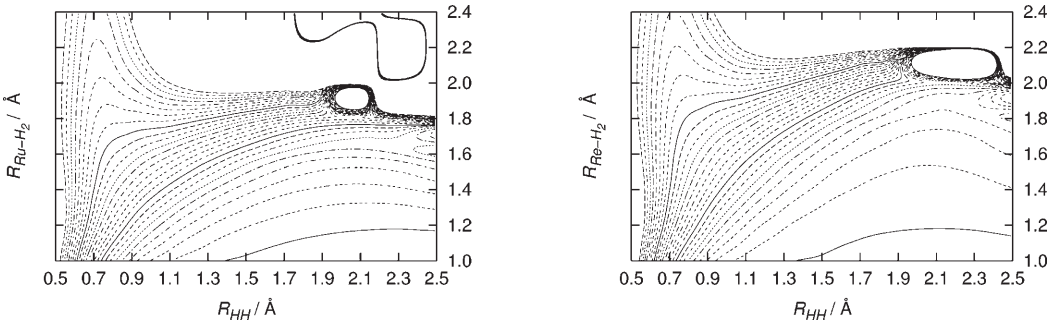

Figure 3. Contour plots of $^1J_{HD}$ for complexes **1′** (left) and **3** (right). Contours start at 2 Hz (contour at bottom right in both cases) and increase in 2 Hz intervals.

tudes at the potential energy minimum of complexes **1′** and **3** where the hydrogen atoms bound to the metal have been described with the IGLO-III basis set.

The improved description of the hydrogen atoms with the IGLO-III basis set did not significantly change either δ or $^1J_{HD}$. In complex **1′**, $\delta = -5.191$ ppm (compared to -5.213 ppm), and for complex **3** $\delta = -5.913$ ppm (compared to -6.057 ppm). As for the spin–spin coupling constants, $^1J_{HD} = 33.3$ Hz in complex **1′** and $^1J_{HD} = 3.45$ Hz in complex **3** (compared to 34.7 Hz and 2.91 Hz, respectively). These results indicate that the results obtained with the smaller basis set are sufficiently converged with respect to the basis set and hence adequate for our present goal.

The final value of $^1J_{HD}$ was obtained as the sum of four different contributions: Fermi contact (FC), spin-dipolar (SD), paramagnetic spin-orbit (PSO), and diamagnetic spin-orbit (DSO). We analyzed the importance of each contribution for complexes **1′** and **3** at the potential energy minimum structures with the IGLO-III basis set. As expected, the main contribution to $^1J_{HD}$ comes from the Fermi contact term (**1′**: +32.9 Hz, **3**: +3.18 Hz). The rest of the contributions are very small (for complex **1′** the three remaining contributions are -0.04 Hz (SO), -0.20 Hz (PSO), and +0.66 Hz (DSO), and for complex **3** the values are +0.02 Hz (SD), -0.18 Hz (PSO), and +0.43 Hz (DSO)).

Dynamical studies: We used DVR to solve the nuclear Schrödinger equation on the PESes of **1′** and **3** for the H–H isotopomer, and computed the expectation values of the geometrical parameters of the M–H_2 unit for the first few vibrational states (Table 3). There is a very clear difference between complex **1′** and **3** in terms of the vibrational wave functions, although there was almost none in terms of the $^1J_{HD}$ and chemical shift surfaces. The probability densities of the first three vibrational states for both complexes are shown in Figure 4. The wave function of the ground state is largely delocalized (i.e. has a nonnegligible amplitude) over a wide range of M–H_2 and H–H distances; however, it is approximately centered on the potential energy minimum for both complexes, thus retaining a general (somewhat elongated) dihydrogen character for **1′** ($\langle R_{H-H}\rangle_{v=0} = 0.99$ Å), and (somewhat compressed) dihydride character for complex **3** ($\langle R_{H-H}\rangle_{v=0} = 1.53$ Å). More quantitatively, the dihydrogen character of either complex in the ground vibrational state can be computed as the integral of the density for the areas of configurational space that correspond to a dihydrogen complex [Eq. (2)],

$$\xi_{\text{dihydrogen}} = \int_0^{+\infty} dR_{M-H_2} \int_0^{+1.0\,\text{Å}} dR_{H-H} |\psi(R_{H-H}, R_{M-H_2})_{v=0}|^2 \quad (2)$$

and analogously, for the dihydride character [Eq. (3)],

$$\xi_{\text{dihydride}} = \int_0^{+\infty} dR_{M-H_2} \int_{+1.5\,\text{Å}}^{+\infty} dR_{H-H} |\psi(R_{H-H}, R_{M-H_2})_{v=0}|^2 \quad (3)$$

This yields a dihydogen character for **1′** of 0.540 in the ground vibrational state, and a dihydride character for **3** of 0.614 in the ground vibrational state.

However, excited states follow quite different patterns. In **1′**, the wave functions of excited vibrational states strongly project to longer H–H (and shorter M–H_2) distances, following the cleft in *U*. As such, increasingly excited states have wave functions that have an amplitude further to the dihydride region. In contrast, complex **3** has excited states that project to shorter H–H distances (and longer M–H_2 distances) also following the cleft in *U*, but this time in the reverse direction. We have applied equations analogous to

Table 3. Vibrational energy levels and expectation values for the geometrical parameters of the M–H_2 unit in complexes **1′** and **3** (H–H isotopomer). Only levels within ≈ 5 kcal mol^{-1} of the vibrational ground state are shown.

State	Complex **1′**			Complex **3**		
	E [kcal mol^{-1}]	$\langle R_{H-H}\rangle$ [Å]	$\langle R_{M-H_2}\rangle$ [Å]	E [kcal mol^{-1}]	$\langle R_{H-H}\rangle$ [Å]	$\langle R_{M-H_2}\rangle$ [Å]
0	4.38	0.99	1.63	3.63	1.53	1.48
1	6.16	1.24	1.53	5.29	1.37	1.53
2	7.48	1.25	1.56	6.86	1.40	1.53
3	8.93	1.27	1.56	8.73	1.43	1.53

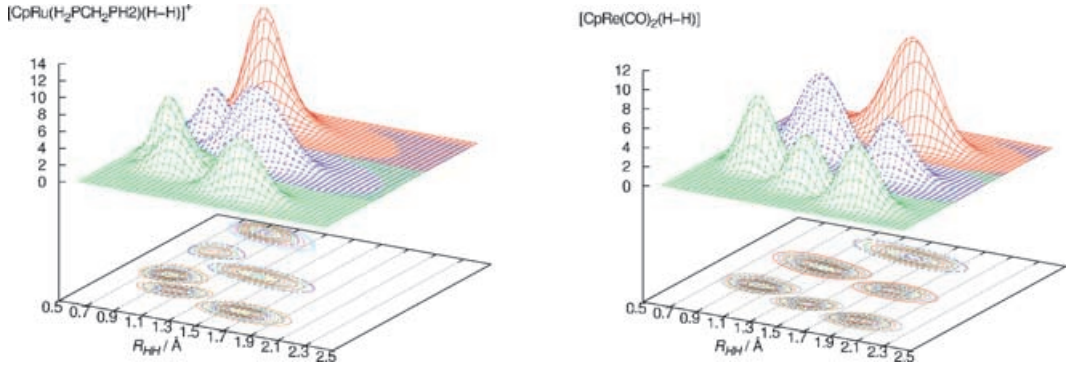

Figure 4. Probability density ($|\psi|^2$) of the vibrational ground state (red), first (blue), and second (green) excited states, for complexes **1′** (left) and **3** (right).

Equation (2) and Equation (3) to quantify the increase of the dihydride character in the vibrational excited states of complex **1′** and of the dihydrogen character in the vibrational excited states of complex **3**, which are represented in Table 4.

Table 4. Dihydride character ($\xi_{dihydride}$) of the vibrational states of complex **1′**, and dihydrogen character ($\xi_{dihydrogen}$) of complex **3** for the lowest vibrational states.

State	$\xi_{dihydride}$ of complex **1′**	$\xi_{dihydrogen}$ of complex **3**
0	0.00776	0.00820
1	0.222	0.119
2	0.383	0.231

We now address complex **1′**: in the immediate vicinity of the potential energy minimum, the path that allows a larger geometric deformation at the least energetic cost is, of course, the cleft in *U*, that is, in the general direction of M–H_2 shortening and H–H lengthening and vice versa. However, because the minimum is *closer* to the dihydrogen region, it is actually easier to *elongate* the H–H bond. Thus, the wave function of the ground state is shifted towards longer H–H distances, and this trend is more evident in excited states. On the contrary, complex **3** has the potential energy minimum in the dihydride region. At that point, it is easier to *shorten* the H–H distance than it is to lengthen it, because lengthening it meets with a continuous rise in energy, whereas shortening it leads to the dihydrogen region, which is low in energy. Not surprisingly, the ground state has an expectation value for the H–H distance that is shorter than at the minimum, and this is true for excited states too. Thus, as the energy of the vibrational state increases, the Ru–H_2 unit is increasingly better described by geometries in the dihydride region, whereas the Re–H_2 unit is better described by structures in the dihydrogen region of the PES.

These different properties should have a direct manifestation in experimentally measurable quantities, such as the isotope effect on the H–H distance, the temperature dependence of the H–H distance, and maybe more easily, $^1J_{HD}$. The isotope effect on the H–H distance reflects the change in the expectation value of R_{H-H} when one considers the HD isotopomer of the complex. To determine this theoretically, we solved the nuclear Schrödinger equation for this isotopomer to find the expectation value for R_{H-H}. Results are presented in Table 5. It can be seen that heavier isotopomers of complex **1′** are predicted to have *shorter* H–H distances, whereas those of complex **3** are predicted to have *longer* H–H distances.

Table 5. Expectation values for R_{H-H} for the HH, HD, and HT isotopomers of complexes **1′** and **3** in the ground vibrational state.

Isotopomer	$\langle R_{H_AH_B}\rangle_{v=0}$ [Å]	
	Complex **1′**	Complex **3**
HH	0.99	1.53
HD	0.96	1.54
HT	0.95	1.55

The temperature dependence of R_{H-H} is easily obtained by determining the expectation values of R_{H-H} for each vibrational state and then carrying out a Boltzmann average at a given temperature. Table 6 contains the values of the thermal averages of R_{H-H} at different temperatures. It can be seen that complex **1′** is predicted to display an *increasing* value of R_{H-H} with temperature, whereas complex **3** is predicted to display the opposite behavior. We note that the present temperature-dependence calculations have been carried out up to 1000 K in order to illustrate the temperature effects, although it is likely that these complexes are not stable at such high temperatures.

Table 6. Thermal average of the H–H distance at different temperatures for complexes **1′** and **3**.

T[K]	$R_{H-H}(T)$[Å]	
	Complex **1′**	Complex **3**
0	0.99	1.53
100	0.99	1.53
200	0.99	1.53
300	1.00	1.52
400	1.02	1.51
500	1.04	1.50
600	1.05	1.49
700	1.07	1.49
800	1.08	1.48
900	1.10	1.47
1000	1.11	1.47

Finally, we address the effects on the $^1J_{HD}$ values. The theoretical estimate of the temperature-dependent $^1J_{HD}$ value is obtained by means of a straightforward Boltzmann average of state-averaged values of $^1J_{HD}$ for individual vibrational states [Eq. 4], where $|\chi_i^{HD}\rangle$ is the *i*th vibrational eigenstate of the M–HD unit, and $^1J_{HD}(R_{H-D}, R_{M-HD},)$ is the computed $^1J_{HD}$ surface (Figure 3).

$$\langle {}^1J_{HD}\rangle_i = \langle \chi_i^{HD}|{}^1J_{HD}(R_{H-D}, R_{M-HD})|\chi_i^{HD}\rangle \quad (4)$$

This requires that the nuclear Schrödinger equation must be solved again for the HD isotopomer to obtain eigenvectors and eigenvalues. State-averaged values for $^1J_{HD}$ are presented in Table 7.

Table 7. Vibrational energy levels and state-averaged values of $^1J_{HD}$ for the HD isotopomers of complexes **1′** and **3**. Only levels within $\approx$5 kcal mol^{-1} of the ground state are shown.

State	Complex **1′**		Complex **3**	
	E [kcal mol^{-1}]	$\langle {}^1J_{HD}\rangle_i$ [Hz]	E [kcal mol^{-1}]	$\langle {}^1J_{HD}\rangle_i$ [Hz]
0	3.68	31.3	3.02	5.1
1	5.29	21.2	4.47	12.0
2	6.34	20.6	5.71	14.0
3	7.50	21.1	7.22	13.2
4	8.71	22.1	7.78	5.7

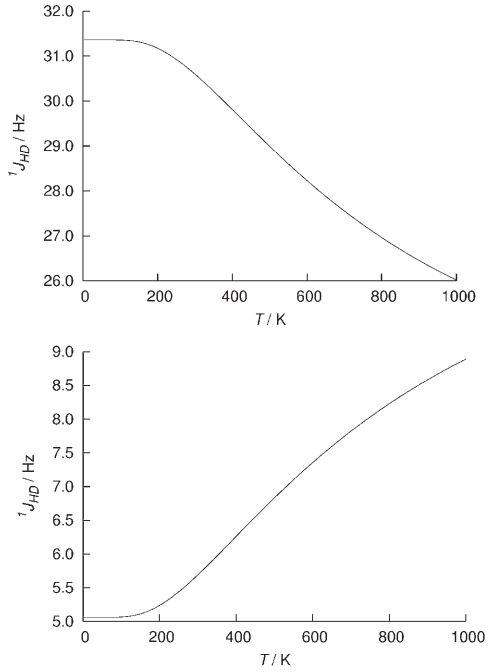

Figure 5. Temperature dependence of $^1J_{HD}$ for complexes **1′** (top) and **3** (bottom).

An inspection of the state-averaged values of $^1J_{HD}$ for the ground and first vibrational excited state of complexes **1′** and **3** (Table 7) indicates that complex **1′** will show decreasing $^1J_{HD}$ with increasing temperature, whereas complex **3** will show increasing $^1J_{HD}$ with increasing temperature for the same reason. Thus, it is not surprising to see such a different behavior confirmed when the Boltzmann average is carried out. Figure 5 shows the Boltzmann average of $^1J_{HD}$ for complexes **1′** and **3**, and it can be clearly seen that complex **1′** shows decreasing, and **3** increasing, $^1J_{HD}$ with temperature; both are in qualitative agreement with experimental data.

Quantitative agreement is excellent for complex **3**: our calculations predict 5.4 Hz at −35 °C and 5.7 Hz at +28 °C (compared to 5.8 Hz and 6.5 Hz, respectively[10]). Quantitative agreement for complex **1′** is not so good, with 30.6 Hz at 295 K and 31.1 Hz at 213 K (compare to 21.1 Hz and 22.3 Hz, respectively[3]). Nonetheless, agreement is much better if one compares the *slope* of $^1J_{HD}(T)$ in the ranges given: for complex **1′**, this is computed to be -6.1×10^{-3} Hz K^{-1}, which compares reasonably well with the experimental value of -15×10^{-3} Hz K^{-1}. For complex **3**, the degree of agreement in terms of this slope is comparable, 4.8×10^{-3} Hz K^{-1} against the experimental value of 11×10^{-3} Hz K^{-1}. We think that these computed values are reasonable, taking into account the many precision-sensitive steps to compute $^1J_{HD}(T)$. We attribute the disagreement in the absolute values of $^1J_{HD}(T)$ for complex **1′** to the electronic structure calculations involved in determining the $^1J_{HD}$ surface, which might more accurately describe the dihydride regions of configurational space rather than those of dihydrogen.

Finally, let us turn our attention to the computation of chemical shift for complexes **1′** and **3**. Heinekey and coworkers found that an isotope shift was measurable: they determined the chemical shift of the dihydrogen ligand to be $\delta_{HH} = -5.975$ ppm at 300 K in CD_2Cl_2.[6] The chemical shifts of the HD isotopomer and the HT isotopomer appeared further upfield by 15 ppb and 22 ppb, respectively. To compare to these data, the state-averaged values of the ^{1}H NMR chemical shift ($\langle\delta\rangle_i$) for the different isotopomers of complex **1′** were computed first (Table 8), followed by the value at 300 K computed through a Boltzmann average. It is enlightening to compare the state-averaged values of the ^{1}H NMR chemical shift for different isotopomers: it is easy to see that these go to higher fields (i.e. to more negative values of δ) for heavier isotopomers. The theoretical value at 300 K for δ_{HH} is −4.516 ppm, which compares well with experimental data. Moreover, δ_{HD} and δ_{HT} are predicted to be 115 and 159 ppb, respectively, upfield from δ_{H-H}. The fact that this method correctly predicts that increasingly heavier isotopomers cause an upfield chemical shift is supportive of the quality of the underlying computational process followed.

Table 8. State-averaged values of the ^{1}H NMR chemical shift for three isotopomers of **1′**. Values for the first few vibrational states are shown.

State	HH		HD		HT	
	E [kcal mol^{-1}]	$\langle\delta\rangle_i$ [ppm]	E [kcal mol^{-1}]	$\langle\delta\rangle_i$ [ppm]	E [kcal mol^{-1}]	$\langle\delta\rangle_i$ [ppm]
0	4.38	−4.550	3.68	−4.679	3.35	−4.733
1	6.16	−3.903	5.29	−4.024	4.83	−4.122
2	7.48	−4.053	6.34	−4.064	5.79	−4.066
3	8.93	−4.016	7.50	−4.067	6.81	−4.098

Casey et al. also found that complex **3** displayed a certain isotope effect on the ^{1}H NMR chemical shift of the hydrides.[10] They found that the hydrides in the HH isotopomer of **3** had a chemical shift of $\delta = -9.240$ ppm in D_8-[toluene] at $T = -34$ °C. The isotope effect for the HD isotopomer at the same temperature was 52 ppb upfield. Table 9 contains the state-averaged values of the chemical shift for complex **3**. An examination of the values of the state-averaged chemical shift shows that the trend seen for complex **1′** does not hold. There are states, such as $\nu = 0$ and $\nu = 1$, where the state-averaged values of the chemical

Table 9. State-averaged values of the ^{1}H NMR chemical shift for two isotopomers of **3**. Values for the first few vibrational states are shown.

State	HH		HD	
	E [kcal mol^{-1}]	$\langle\delta\rangle_i$ [ppm]	E [kcal mol^{-1}]	$\langle\delta\rangle_i$ [ppm]
0	3.63	−6.019	3.00	−6.015
1	5.29	−6.565	4.47	−6.521
2	6.86	−6.632	5.71	−6.708
3	8.73	−6.556	7.22	−6.616

shift are slightly further upfield for the HH isotopomer, contrary to what has been computed for complex **1′**, whereas there are other states for which the reverse behavior holds. This is a consequence of the shape of the cleft in the potential energy surface being almost parallel to the isolines in the $\delta(R_{H-H},R_{M-H_2})$ surface, which makes the vibrational wave functions extend mostly over areas where the chemical shift is approximately constant, and thus, state-averaged values of it are almost indistinguishable, even for different isotopic compositions.

Through use of a Boltzmann average, the thermal averages of the chemical shift for the HH and HD isotopomers can be computed along with the isotope effect on the chemical shift. We find that this isotope effect is 4 ppb upfield for the HD isotopomer at $T = -34\,^{\circ}C$. It is predicted that the HD isotopomer will have a chemical shift further upfield than the HH isotopomer, which is also in agreement with the available data.

Fundamental differences between elongated dihydrogen and compressed dihydride complexes: In this study, and from a comparison with data reported elsewhere for complex **2**,[9] we have found a striking similarity between the $^1J_{HD}$ and δ surfaces for different complexes. This indicates that no significant differences exist at the electronic structure level as far as these parameters are considered *when comparing equivalent configurations*. The very different properties observed experimentally, and correctly predicted with our theoretical calculations, arise from 1) where the ground vibrational wave function has largest amplitude, and 2) where the first few vibrational states' wave functions have largest amplitudes. Point 1 provides information on the principal characteristics of the complex, while point 2 provides information on the temperature dependence of these characteristics. Both points are connected.

Take complex **1′** as a representative of elongated dihydrogen complexes with a short H–H distance: in this case, the vibrational analysis has revealed that 1) the wave function of the vibrational ground state extends over a wide area but spreads preferentially towards areas corresponding to *longer* H–H distances, and 2) the wave functions of the first vibrational excited states have larger amplitudes towards areas described by increasing dihydride (longer H–H) character. As a result, point 1 makes this complex display $^1J_{HD}$ values that are generally large (closer to what is expected for dihydrogen complexes), and in any case, causes the complex to have a geometry with longer H–H distances than those of the potential energy minimum, and point 2 makes the dihydride character increase with temperature, that is, makes $^1J_{HD}$ decrease with temperature.

An analogous reasoning can be applied to complexes **3** (this work) and **2**.[9] In these cases, the vibrational analysis reveals that 1) the wave function of the vibrational ground state has a larger amplitude in regions of configurational space where the H–H distance is shorter than in the minimum, and 2) the wave functions of the first vibrational excited states extend towards areas described by increasing dihydrogen (shorter H–H) character. Similarly, point 1 makes these complexes display $^1J_{HD}$ values that are generally small (closer to what is expected for dihydride complexes), with a geometry that is slightly shorter than that of the potential energy minimum. Point 2, in sharp contrast to complexes such as **1′**, makes the dihydrogen character increase with temperature, that is, makes $^1J_{HD}$ increase with temperature.

Complexes **1′** and **3** differ essentially in the topology of their potential energy surfaces, not in the topology of their $^1J_{HD}$ or δ surfaces. We have demonstrated that these different topologies, in terms of where the absolute minimum is and in what direction from the minimum it is less costly to modify the H–H distance, determine clearly where the ground vibrational state is centered and the direction in which the vibrational excited states project. We have also shown that this uniquely determines the range of values of $^1J_{HD}$ and their temperature dependence, which is clearly different, depending on whether a short H–H distance minimum (decreasing $^1J_{HD}$ with temperature) or a long H–H distance minimum (increasing $^1J_{HD}$ with temperature) is present. The clearly different properties in topological terms of the potential energy surface then find a *dynamical* measurable effect in terms of the isotope effect on the H–H distance, the temperature dependence of the H–H distance, and the temperature dependence of $^1J_{HD}$.

Accordingly, we think that complexes such as **1′** and **3** *can* be distinguished as chemical species, similar indeed but differentiable by means of a single experimental test: establishing the sign of the temperature dependence of $^1J_{HD}$, and, as such, can be properly identified by different names. Complex **1′** is more similar to a dihydrogen complex, with a longer expectation value for the H–H distance, and upon increasing temperature its dihydride character increases. Hence the usual name *stretched dihydrogen complex* is very reasonable. Complexes **2** and **3** are more similar to dihydride complexes, with a shorter expectation value of the H–H distance than that of their potential energy minimum, and upon increasing the temperature dependence their dihydrogen character increases. In our opinion, the name *compressed dihydride complex* is justifiable in these cases.

One puzzling question remains unanswered: some time ago, Morris and co-workers reported a thorough experimental study of complex *trans*-$[Os(H_2)Cl(dppe)_2]PF_6$ (**5**).[35] A H–H distance of 1.22(3) Å was determined by single-crystal neutron diffraction in the solid state. Variable-temperature solution ^{1}NMR experiments revealed that the magnitude of $^1J_{HD}$ increased with temperature, a novel behavior at that time for elongated dihydrogen complexes. It was also established that the librational motion of the dihydrogen ligand was mostly unhindered. In a theoretical study of complex *trans*-$[Os(H_2)Cl(H_2PCH_2CH_2PH_2)_2]PF_6$ (**5′**), taken as a simplified model of **5**,[29] we found that the potential energy surface at the DFT level was flatter and more anharmonic than that of complex **1′**. A nuclear dynamics calculation on the 2-dimensional potential energy surface constructed in the same way as in this work yielded a good description for the expected geometry in the ground vibrational state (1.20 Å),

but also predicted a steady increase of the mean thermal R_{H-H} distance with temperature, in disagreement with experimental data. Inclusion of a third degree of freedom describing the librational motion of the dihydrogen ligand, which explicitly considered the dependence of the librational barrier on R_{H-H}, improved the description of the expectation value of the H–H distance for the ground state (1.23 Å) and predicted the existence of a certain range of temperatures in which the actual H–H distance would decrease. Thus, the tentative explanation of the experimental behavior attributed this to the influence of the librational motion of the H–H ligand. Recently, Gusev has found that in complex **5** significant interaction might happen between the dihydrogen ligand and the counterion, thus suggesting that the crystal structure of **5** is different from that of the corresponding cation when ion pairing is not present.[36] In fact, the potential energy surface for complex **5′** was found to be extremely flat (stretching the H–H bond from 1.0 Å to 1.5 Å implied an energy change of only 0.5 kcal mol^{-1})[29] so it seems possible that otherwise weak interactions, such as ion-pairing, might have an effect in this case that would go unnoticed otherwise. As such, the implication of the librational motion of the H–H unit in the inverse temperature dependence of $^1J_{HD}$ should be regarded as inconclusive.

Conclusions

With the aim of discerning the existence of "compressed dihydride complexes" as different entities from elongated dihydrogen complexes, a thorough comparative theoretical study has been undertaken on complexes $[Cp^*Ru(dppm)(H_2)]^+$ (R_{H-H} = 1.10 Å, neutron diffraction[3]) and $[CpRe(CO)_2H_2]$ (R_{H-H} = 1.41 Å, $^1J_{HD}$ data[10]), including quantum dynamics calculations and computation of the dependence of $^1J_{HD}$ on the temperature from first principles, that is, without resorting to correlations of any kind.

It has been found that both complexes share striking similarities as far as the $^1J_{HD}$ and ^{1}H NMR chemical shift for the dihydrogen ligand are concerned, and that this similarity holds when comparing to another case recently studied, $[Cp^*Ir(dmpm)H_2]^{2+}$.[8] Actually, the main difference comes from the location of the potential energy minimum *and* the direction of least energetic cost upon deformation of the H–H distance. Those complexes with a minimum closer to dihydrogen-type distances have *larger* $^1J_{HD}$ values in general and, importantly, display *decreasing* $^1J_{HD}$ with temperature. Conversely, complexes with a minimum closer to dihydride-type distances generally have *smaller* $^1J_{HD}$ values and should show *increasing* $^1J_{HD}$ values with temperature.

Two different families of complexes can be seen comprising the elongated or stretched dihydrogen complex group. On the one hand, the elongated dihydrogen complexes themselves, which 1) should have their potential energy minimum close to the dihydrogen minimum, thus having a strong dihydrogen character, such as large $^1J_{HD}$ values in general, and 2) will increase their dihydride character with temperature, showing decreasing $^1J_{HD}$ with temperature and increasing R_{H-H} with temperature. Complex $[Cp^*Ru(dppm)(H_2)]^+$ belongs to this group. On the other hand, compressed dihydride complexes would differ from the previously described because 1) they have their potential energy minimum in the dihydride region, thus having a strong dihydride character, such as small $^1J_{HD}$ values in general, and 2) they will increase their dihydrogen character with temperature, showing increasing $^1J_{HD}$ with temperature and decreasing R_{H-H} with temperature. Complexes $[CpRe(CO)_2H_2]$ and $[Cp^*Ir(dmpm)H_2]^{2+}$ would fit this description. Both kinds of complexes should show isotope geometric effect when the HH unit is substituted by heavier types, such that the R_{H-H} distance would be decreased in elongated dihydrogen complexes and increased in compressed dihydride complexes.

Thus, the elongated (or stretched) dihydrogen and compressed dihydride complexes should be distinguishable by means of any of three experimental measurements in which they are predicted to show opposing behavior: 1) isotope effect on R_{H-H}, 2) temperature dependence of R_{H-H}, and 3) temperature dependence of $^1J_{HD}$.

Acknowledgements

R.G. acknowledges the Spanish "Ministerio de Ciencia y Tecnología" for a "Ramón y Cajal" research contract. The authors are grateful for financial support from the Spanish "Ministerio de Ciencia y Tecnología" and the "Fondo Europeo de Desarrollo Regional" through project BQU2002–00301. The use of computational facilities at the "Centre de Supercomputació de Catalunya" is acknowledged.

[1] D. M. Heinekey, A. Lledós, J. M. Lluch, *Chem. Soc. Rev.* **2004**, *33*, 175–182.
[2] S. Gründemann, H. H. Limbach, G. Buntkowsky, S. Sabo-Etienne, B. Chaudret, *J. Phys. Chem. A* **1999**, *103*, 4752–4754.
[3] W. T. Klooster, T. F. Koetzle, G. C. Jia, T. P. Fong, R. H. Morris, A. Albinati, *J. Am. Chem. Soc.* **1994**, *116*, 7677–7681.
[4] R. Gelabert, M. Moreno, J. M. Lluch, A. Lledós, *J. Am. Chem. Soc.* **1997**, *119*, 9840–9847.
[5] J. K. Law, H. Mellows, D. M. Heinekey, *J. Am. Chem. Soc.* **2001**, *123*, 2085–2086.
[6] J. K. Law, H. Mellows, D. M. Heinekey, *J. Am. Chem. Soc.* **2002**, *124*, 1024–1030.
[7] V. Pons, D. M. Heinekey, *J. Am. Chem. Soc.* **2003**, *125*, 8428–8429.
[8] R. Gelabert, M. Moreno, J. M. Lluch, A. Lledós, V. Pons, D. M. Heinekey, *J. Am. Chem. Soc.* **2004**, *126*, 8813–8822.
[9] R. Gelabert, M. Moreno, J. M. Lluch, A. Lledós, D. M. Heinekey, *J. Am. Chem. Soc.* **2005**, *127*, 5632–5640.
[10] C. P. Casey, R. S. Tanke, P. N. Hazin, C. R. Kemnitz, R. J. McMahon, *Inorg. Chem.* **1992**, *31*, 5474–5479.
[11] L. Torres, M. Moreno, J. M. Lluch, *J. Phys. Chem. A* **2001**, *105*, 4676–4681.
[12] M. J. Frisch, G. W. Trucks, H. B. Schlegel, G. E. Scuseria, M. A. Robb, J. R. Cheeseman, J. A. Montgomery, Jr., T. Vreven, K. N. Kudin, J. C. Burant, J. M. Millam, S. S. Iyengar, J. Tomasi, V. Barone, B. Mennucci, M. Cossi, G. Scalmani, N. Rega, G. A. Petersson, H. Nakatsuji, M. Hada, M. Ehara, K. Toyota, R. Fukuda, J. Hasegawa, M. Ishida, T. Nakajima, Y. Honda, O. Kitao, H. Nakai, M. Klene, X. Li, J. E. Knox, H. P. Hratchian, J. B. Cross, C. Adamo, J. Jaramillo, R. Gomperts, R. E. Stratmann, O. Yazyev, A. J. Austin, R.

Cammi, C. Pomelli, J. W. Ochterski, P. Y. Ayala, K. Morokuma, G. A. Voth, P. Salvador, J. J. Dannenberg, V. G. Zakrzewski, S. Dapprich, A. D. Daniels, M. C. Strain, O. Farkas, D. K. Malick, A. D. Rabuck, K. Raghavachari, J. B. Foresman, J. V. Ortiz, Q. Cui, A. G. Baboul, S. Clifford, J. Cioslowski, B. B. Stefanov, G. Liu, A. Liashenko, P. Piskorz, I. Komaromi, R. L. Martin, D. J. Fox, T. Keith, M. A. Al-Laham, C. Y. Peng, A. Nanayakkara, M. Challacombe, P. M. W. Gill, B. Johnson, W. Chen, M. W. Wong, C. Gonzalez, J. A. Pople, GAUSSIAN 03, Revision B.04, Gaussian, Inc., Pittsburgh PA (USA), **2003**.

[13] R. G. Parr, W. Yang, *Density Functional Theory of Atoms and Molecules*, Oxford University Press, Oxford, UK, **1989**.
[14] T. Ziegler, *Chem. Rev.* **1991**, *91*, 651–667.
[15] C. T. Lee, W. T. Yang, R. G. Parr, *Phys. Rev. B* **1988**, *37*, 785–789.
[16] A. D. Becke, *J. Chem. Phys.* **1993**, *98*, 5648–5652.
[17] P. J. Hay, W. R. Wadt, *J. Chem. Phys.* **1985**, *82*, 299–310.
[18] A. Hollwarth, M. Bohme, S. Dapprich, A. W. Ehlers, A. Gobbi, V. Jonas, K. F. Kohler, R. Stegmann, A. Veldkamp, G. Frenking, *Chem. Phys. Lett.* **1993**, *208*, 237–240.
[19] M. M. Francl, W. J. Pietro, W. J. Hehre, J. S. Binkley, M. S. Gordon, D. J. Defrees, J. A. Pople, *J. Chem. Phys.* **1982**, *77*, 3654–3665.
[20] W. J. Hehre, R. Ditchfield, J. A. Pople, *J. Chem. Phys.* **1972**, *56*, 2257–2257.
[21] P. C. Hariharan, J. A. Pople, *Theor. Chim. Acta* **1973**, *28*, 213–222.
[22] R. McWeeny, *Phys. Rev.* **1962**, *126*, 1028–1028.
[23] R. Ditchfield, *Mol. Phys.* **1974**, *27*, 789–807.
[24] K. Wolinski, J. F. Hinton, P. Pulay, *J. Am. Chem. Soc.* **1990**, *112*, 8251–8260.
[25] V. Barone, J. E. Peralta, R. H. Contreras, J. P. Snyder, *J. Phys. Chem. A* **2002**, *106*, 5607–5612.
[26] V. Sychrovsky, J. Gräfenstein, D. Cremer, *J. Chem. Phys.* **2000**, *113*, 3530–3547.
[27] T. Helgaker, M. Watson, N. C. Handy, *J. Chem. Phys.* **2000**, *113*, 9402–9409.
[28] W. Kutzelnigg, U. Fleischer, M. Schindler, *The IGLO-Method: Ab Initio Calculation and Interpretation of NMR Chemical Shifts and Magnetic Susceptibilities*, *Vol. 23*, Springer, Heidelberg, **1990**.
[29] R. Gelabert, M. Moreno, J. M. Lluch, A. Lledós, *J. Am. Chem. Soc.* **1998**, *120*, 8168–8176.
[30] R. Gelabert, M. Moreno, J. M. Lluch, A. Lledós, *Chem. Phys.* **1999**, *241*, 155–166.
[31] W. H. Press, B. P. Flannery, S. A. Teukolsky, W. T. Vetterling, *Numerical Recipes in Fortran*, *2nd ed.*, Cambridge University Press, Cambridge, UK, **1992**.
[32] D. T. Colbert, W. H. Miller, *J. Chem. Phys.* **1992**, *96*, 1982–1991.
[33] T. Helgaker, M. Jaszunski, K. Ruud, *Chem. Rev.* **1999**, *99*, 293–352.
[34] J. Vaara, J. Jokisaari, R. E. Wasylishen, D. L. Bryce, *Prog. Nucl. Magn. Reson. Spectrosc.* **2002**, *41*, 233–304.
[35] P. A. Maltby, M. Schlaf, M. Steinbeck, A. J. Lough, R. H. Morris, W. T. Klooster, T. F. Koetzle, R. C. Srivastava, *J. Am. Chem. Soc.* **1996**, *118*, 5396–5407.
[36] D. G. Gusev, *J. Am. Chem. Soc.* **2004**, *126*, 14249–14257.

Received: March 14, 2005
Published online: August 1, 2005

